

Direct Observation of the Orientation Dynamics of Single Protein-Coated Nanoparticles at Liquid/Solid Interfaces**

Dong Xu, Yan He,* and Edward S. Yeung

Abstract: We have observed the rotational dynamics of single protein-coated gold nanorods (AuNRs) on C_{18} -modified silica surfaces in real time by dual-channel polarization dark-field microscopy. Four different rotational states were identified, depending on the apparent strength of interactions between the AuNRs and the surface. The distributions of the states could be regulated by adjusting the salt concentration, and the state transitions were verified by monitoring the entire desorption process of a single AuNR. Our study provides insight into the interfacial orientation and dynamics of nanoparticles and could be useful for in vitro biophysics and the separation of proteins.

Characterization of the dynamics of individual molecules or nanoparticles (NPs) at liquid/solid interfaces is highly important in diverse areas, including chemical, biomedical, materials, and separation science.^[1] Toward this goal, optical-imaging-based single-molecule tracking (SPT) techniques have been developed to monitor interactions between individual molecules and functionalized surfaces.^[2] From spatial and temporal distributions of physical properties, such as the intensity, spectrum, residence time, trajectory, and diffusion coefficient, new knowledge on interfacial mechanisms can be revealed.^[3] However, previous SPT studies on chemically modified solid surfaces have focused mostly on translational diffusion of the probes. In reality, interfacial dynamics involve not only translational but also rotational motions of the molecules. It was reported that the reorientation and rotation of dye molecules were restricted on C_{18} -modified silica surfaces.^[4] To enable deeper understanding and better control of liquid/solid interfacial events, it is desirable to monitor the rotational behavior of individual probes at interfaces in real time.

One essential interfacial problem is the interaction between proteins and solid surfaces, which is a fundamental issue in biophysics and the separation of proteins. For example, in hydrophobic interaction chromatography (HIC), a widely used protein-purification method, it is

generally recognized that the hydrophobic patches on the protein-molecule surface interact nonspecifically and reversibly with the hydrophobic ligands on the stationary-phase surface in the presence of kosmotropic salts, such as ammonium sulfate. Protein unfolding and adsorption are induced by a high salt concentration, and protein refolding and desorption are promoted at a low salt concentration.^[5] These conformational changes are usually accompanied by variations in the orientation and rotational state of the proteins,^[6] but their time scales are too short for existing 2D image detectors.

Owing to their anisotropic shape-induced optical properties, large scattering/absorption cross-section, and high photostability, single gold nanorods (AuNRs) have become popular probes for rotational and orientation sensing.^[7] By exploitation of their polarization-sensitive longitudinal localized surface plasmon resonance (LSPR), dark-field microscopy, differential interference contrast microscopy, and photothermal imaging have been developed to determine the 2D or 3D orientation angles of single AuNRs.^[8] In this study, by dual-channel polarization dark-field microscopy (DPDFM), we monitored the orientation dynamics of AuNRs coated with bovine serum albumin (BSA) on C_{18} -modified silica surfaces. It was found that protein-coated AuNRs behave like large artificial molecules and undergo slow reorientation and rotation during adsorption/desorption on C_{18} surfaces, thus allowing different AuNR orientation states and transitions to be observed in situ on a millisecond time scale under typical HIC separation conditions. The concepts derived from HIC were used to interpret the surface interactions with the AuNRs. Our results could provide new insight into NP orientation and dynamics at surfaces, such as the self-assembly of nanoparticles into organized arrays.

The optical setup of DPDFM (Figure 1a) is similar to previously reported setups.^[7a,8c] Briefly, by the use of a low numerical aperture objective and a birefringent prism for light collection, the LSPR scattering of each AuNR is split into two channels with orthogonal polarization, that is, $I_X \propto \sin^2\theta \cos^2\phi$ and $I_Y \propto \sin^2\theta \sin^2\phi$, in which θ is the polar angle and ϕ is the azimuth angle of the AuNR (Figure 1b). Hence the ϕ value can be readily calculated from the intensity difference of the two channels, $(I_X - I_Y)/(I_X + I_Y) \approx \cos(2\phi)$, and the θ value can be obtained from the intensity sum of the two, $I_{\text{sum}} = I_X + I_Y \propto \sin^2\theta$. In the particular case of dark-field microscopy with annular inclined illumination, the contribution of ϕ to I_{sum} is nullified owing to integration of the incident light over 0 to 2π ; thus, I_{sum} is a monotonic function of θ (see Figure S1 in the Supporting Information).^[9] Hence, the variation of I_{sum} can be used to characterize the out-of-plane angle of the AuNR relative to the surface.^[9b]

[*] D. Xu, Prof. Dr. Y. He, Prof. Dr. E. S. Yeung
State Key Laboratory of Chemo/Biosensing and Chemometrics,
College of Chemistry and Chemical Engineering, College of Biology
Hunan University
Changsha, 410082 (P. R. China)
E-mail: yanhe2021@gmail.com

[**] This research was supported by NSFC grant 21127009, NSFC grant 91027037, NSFC grant 21221003, and the Hunan University 985 Fund.



Supporting information for this article is available on the WWW under <http://dx.doi.org/10.1002/anie.201400025>.

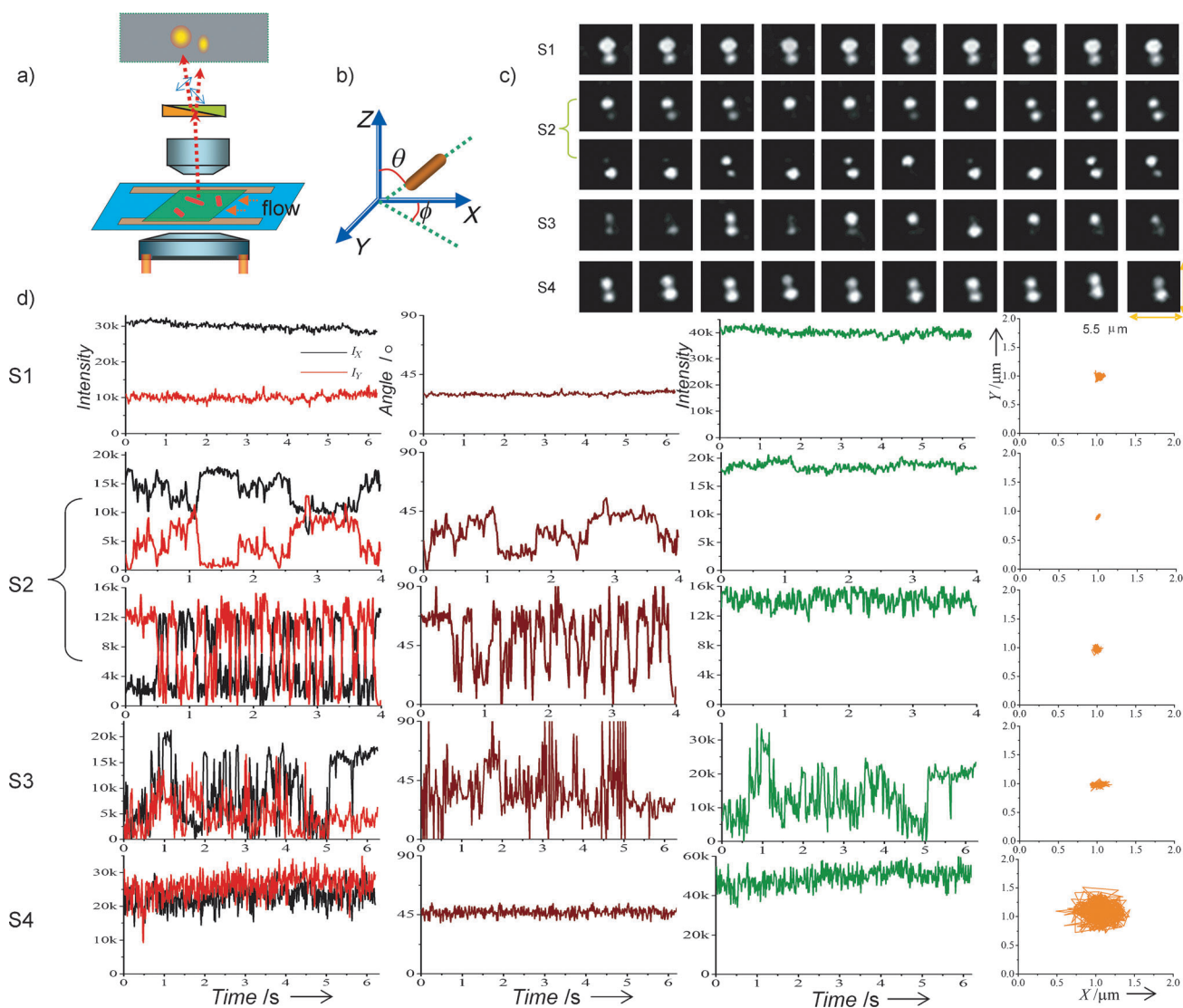


Figure 1. Different dynamic states observed by dual-polarization dark-field microscopy. a) Schematic diagram of the optical setup. b) Coordinate system. c) Typical image sequences of single AuNRs in different dynamic states. d) Time-dependent variations of I_x and I_y , the calculated azimuth angle, and I_{sum} , and the trajectories of the four dynamic states (from left to right).

The preparation and characterization of the BSA-coated $70 \times 32 \text{ nm}^2$ AuNRs (see Figure S2) as well as the C_{18} -silanized silica surfaces (see Figure S3) are described in detail in the Supporting Information. To verify the existence of hydrophobic interactions between the as-prepared AuNRs and the substrate, we obtained DFM images of α -amylase-coated and BSA-coated AuNRs at the same concentration in water and in $1.7 \text{ M } (\text{NH}_4)_2\text{SO}_4$ aqueous solution on either the bare silica surface or the C_{18} surface. α -Amylase is a protein much more hydrophobic than BSA, and a very high concentration of salt is known to make the protein molecules swiftly unfold so that the interior hydrophobic pockets are fully exposed to the C_{18} ligands.^[10] In all cases, α -amylase-coated AuNRs were more readily adsorbed than BSA-coated AuNRs (see Figure S4), thus indicating that the hydrophobicity of the modified AuNRs is determined by the protein coat. Furthermore, for both types of AuNRs, the amount of particles adsorbed on the C_{18} surface was always higher than on the silica surface, thus

indicating that the AuNRs can differentiate the two surfaces in terms of their hydrophobicity. Finally, upon an increase in the salt concentration, both AuNRs were more readily adsorbed, a phenomenon consistent with that observed for pure proteins. It is known that $(\text{NH}_4)_2\text{SO}_4$ binds water strongly; raising the concentration of the salt decreases charge shielding, promotes exposure of the hydrophobic patches both in the molecules and on the stationary phase, results in increased hydrophobic affinity between the molecules and the stationary phase, and promotes the unfolding of proteins from their native state.^[11] A recent study on the structure of BSA molecules absorbed on AuNRs with synchrotron radiation X-ray absorption spectroscopy and molecular dynamics simulations showed that the proteins undergo only partial spreading after AuNR binding, and that their structural flexibility is preserved, thus implying that they can still respond to the local environment change.^[12] Hence, although the protein-coated AuNRs are quite large, their

interfacial behavior is similar to that of proteins alone, so they can be treated as large artificial semielastic molecules for the purpose of protein–surface interaction studies.

Figure 1c shows typical DPDFM image sequences of single AuNRs on the C_{18} surface when an aqueous $(NH_4)_2SO_4$ solution at a constant concentration of 0.85–0.7 M was applied (see also Movie 1 in the Supporting Information). Four different dynamic states, that is, fixation (S1), in-plane rotation (S2), out-of-plane rotation (S3), and delocalized Brownian rotation (S4), apparently corresponding to the decreasing affinity of the BSA layer for the C_{18} surface, were observed. The typical time-dependent variations in the I_X , I_Y , ϕ , and I_{sum} values, as well as the trajectories of the four states, are exhibited in Figure 1D (see Movie 2 and Figure S5 for more results).

S1 is the state in which the AuNR is completely immobilized on the surface, and neither translational nor rotational motion of the AuNRs can be detected. In this case, there is little variation in I_X , I_Y , and I_{sum} , and thus in ϕ and θ , but the magnitudes of I_X and I_Y are generally not the same owing to the random orientation of each dipole on the surface. Such a state is attributed to strong binding of the protein-coated AuNR to the C_{18} surface, presumably through multiple anchoring points.

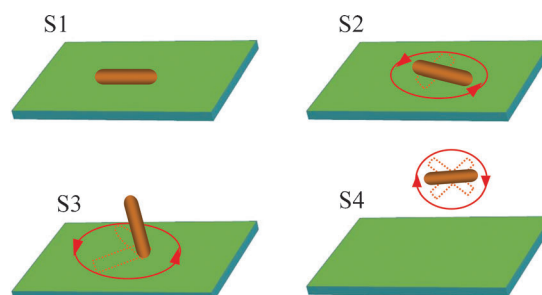
S2 is the state in which the AuNR is adsorbed at one position on the surface but not very tightly. In this case, there are clear time-dependent variations in I_X or I_Y , but I_{sum} remains nearly constant, that is, ϕ changes with time, but θ does not. Hence, S2 is the state in which the AuNR undergoes in-plane rotation while remaining stationary. Depending on the relative values of I_X and I_Y , S2 can be further divided into two regimes: one in which the intensity fluctuation is not too large, so that the variation in ϕ is small, and another in which I_X and I_Y both fluctuate widely, while I_{sum} remains unchanged, thus resulting in large variations in ϕ but not θ . In either situation, the affinity of the BSA-coated AuNR for the binding site cannot be very strong. At least two points on the BSA layer are probably always in contact with the C_{18} surface, even though that may involve desorption and readsorption, thereby allowing twisting or rotation of the nanorod parallel to the C_{18} surface.

S3 is the state in which the AuNR is able to rotate in three dimensions but is still loosely confined to the surface. Whereas the lateral position of the AuNR remains unchanged, both scattering spots appear to flicker independently. The fluctuations of I_X and I_Y are uncorrelated with time, and I_{sum} is not steady any longer, thus implying that the polar angle is changing, and that the AuNR is flipping or rotating out of the plane. In this case, the affinity between the BSA layer and the C_{18} ligands is weak. It is barely strong enough to hold the AuNR on site and reduce its rotational motion. As a result, the nanorod continuously taps the adsorption site at various orientations; that is, single-point adsorption to the surface probably occurs.

S4 is the state in which the AuNR detaches from the C_{18} surface but still remains in the vicinity of the adsorption site. The nanorod is observed to diffuse laterally near the surface and could eventually go further into the bulk solution (becoming out of focus). Because it is in solution, the

rotational diffusion constant of the AuNR ($1.2 \times 10^4 \text{ s}^{-1}$ in theory) is very fast as compared to the exposure time of the camera. Therefore, the detected intensities I_X and I_Y are nearly identical, thus leading to an average ϕ value of 45° . In this case, the AuNR is probably weakly held by the long-range electrostatic and hydrophobic interactions with the surface.^[13]

Overall, these four dynamic states can be readily differentiated qualitatively according to the relative variations of the azimuth angle, the summed intensity, and the lateral positions of the AuNRs (Figure 2). An alternative semi-



State	ϕ variation	I_{sum} variation	XY position
S1	N	N	N
S2	Y	N	N
S3	Y	Y	N
S4	Y*	Y*	Y

Figure 2. Schematic diagrams of the four dynamic states of AuNRs and their differentiation criteria (N=no, Y=yes). The ϕ and I_{sum} values in S4 appear invariant owing to the extremely fast rotation of AuNRs in solution.

quantitative approach based on correlation analysis of I_X and I_Y to identify different rotational modes of AuNRs on membrane surfaces^[14] was not applicable in our situations (see Table S1 in the Supporting Information). From S1 to S4, the apparent strength of the hydrophobic interaction between the BSA-coated AuNRs and the C_{18} surface decreases. Since the bulk solution environment is homogeneous, the emergence of these various states at the same liquid/solid interface must stem from the heterogeneity of the solid surface as a result of defects, patterning, and roughness of the C_{18} layer. The assembly of the protein coating and the topography of the nanorod surface may also affect the behavior of individual AuNRs as a function of their spatial location. Consequently, heterogeneous interfacial molecular dynamics is inevitable. As the three states S1, S2, and S3 differ only in the rotational behavior of the AuNR, they would appear degenerate if only the AuNR translational diffusion was monitored. Hence, single-particle rotational tracking provides more detailed information on the dynamics of adsorbate/interface interactions.

To confirm that the four dynamic states are closely related to the chromatographic separation of the solute molecules, the distributions of the four states observed under HIC elution conditions with different salt concentrations were studied. Above a 0.9 M concentration of $(NH_4)_2SO_4$, 100% of the AuNRs were in the S1 state. We started to observe

significant rotation of the AuNRs when the concentration was reduced below 0.9 M. Below 0.5 M, more than 75 % of the AuNRs were flushed away. Figure 3 shows the histograms obtained by examining hundreds of the AuNRs (according to

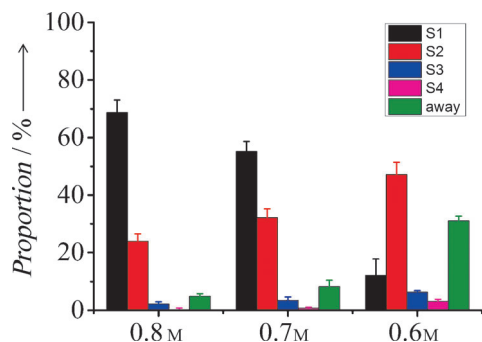


Figure 3. Distributions of the dynamic states in the presence of $(\text{NH}_4)_2\text{SO}_4$ at concentrations of 0.8, 0.7, and 0.6 M.

the criteria in Figure 2) in the presence of 0.8, 0.7, and 0.6 M $(\text{NH}_4)_2\text{SO}_4$. Besides the distribution of the four states, the AuNRs that were flushed away from the adsorption site and disappeared from the images were also counted. At 0.8 M $(\text{NH}_4)_2\text{SO}_4$, 69 % of the AuNRs remained in the S1 state, 24 % were in the S2 state, and just 5 % were released from the surface. However, at 0.6 M $(\text{NH}_4)_2\text{SO}_4$, only 12 % of the AuNRs were in the S1 state, 47 % were in the S2 state, and 31 % went away (see Movie 3). The population of the S2, S3, and S4 states all increased relative to that of S1 as the $(\text{NH}_4)_2\text{SO}_4$ concentration decreased. The number of AuNRs that remained in the in-plane rotation mode was quite large; hence, S2 was a metastable state that even became the primary state at a 0.6 M concentration of the salt. The states S3 and S4 are stochastic rare events that were observed only intermittently. Similar results were obtained when the AuNR protein coating was replaced with trypsin or histone, although the critical $(\text{NH}_4)_2\text{SO}_4$ concentrations that caused the AuNRs to start to rotate were not the same. These results indicated that the desorption of the protein-coated AuNRs from the C_{18} surface is sensitive to variations in the salt concentration, and their counts and residence times at different intermediate states may be applied to evaluate chemically modified surfaces.

Besides identifying different interfacial behaviors in spatially distinct AuNRs under equilibrium conditions, we also observed unsynchronized dynamic state transitions of the same AuNRs from S1 to S4 under typical chromatographic conditions. Figure 4 depicts the entire desorption process of a single BSA-coated AuNR under continuous elution with 0.6 M $(\text{NH}_4)_2\text{SO}_4$ (see also Movie 4). Before 1.14 s after the eluent was applied, the surface-adsorbed AuNR was motionless in state S1. The AuNR then made a sudden in-plane twist and came back immediately. After approximately 0.8 s, it made another two consecutive in-plane twists for 0.08 and 0.05 s, respectively. After pausing for approximately 0.3 s, with a slight increase in angular fluctuation, the AuNR made a one-way in-plane rotation, and its dynamic state changed from S1 to S2, whereby both I_x and I_y started to fluctuate

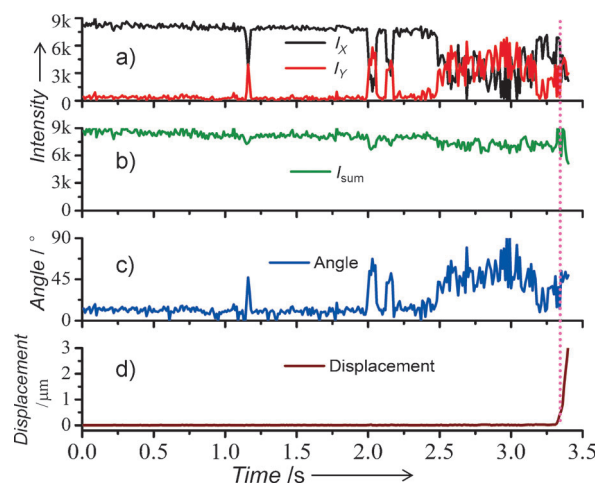


Figure 4. Time-dependent variation of a) the I_x and I_y value, b) the I_{sum} value, c) the azimuth angle, and d) the lateral displacement of a single BSA-coated AuNR in 0.6 M aqueous $(\text{NH}_4)_2\text{SO}_4$ during its entire desorption process under flow.

considerably, and I_{sum} remained about the same. At 3.32 s, the AuNR started to detach from the surface site with increasing fluctuation of the I_{sum} value and a ϕ value close to 45° , thus indicating that it entered the S4 state. Finally, after 3.4 s, the AuNR moved away from the surface, whereupon its image became defocused. The S3 state was not observed in this case, probably because the shear force of the flow did not allow on-site out-of-plane rotation of the nanorod. Nevertheless, it can be seen that the AuNR delocalization or detachment from the surface is not an instantaneous process and is preceded by a series of orientation adjustments as well as in-plane or out-of-plane rotations, as may be the case for most macromolecules. More studies are under way to determine whether this behavior is a general rule. The added temporal information for individual AuNRs, on the time scale of their actual reorientation “steps”, provides new details about the interactions between the adsorbate and the C_{18} surface.

In summary, we successfully monitored the orientation dynamics of protein-coated single AuNRs on C_{18} -modified silica surfaces by using DPDFM. Four different states corresponding to decreasing affinity of the nanorods for the hydrophobic surface were identified. The distribution of these states varied with the $(\text{NH}_4)_2\text{SO}_4$ concentration. A real-time study of dynamic state transitions implies that the dislocation of elastic adsorbates is preceded by in-plane rotation and orientation adjustment. Although these AuNRs are much larger and rotate much more slowly than a protein molecule, their interfacial dynamics comprise the collective structural changes of all the adsorbed but still flexible proteins and involve variations of the surface contact points as well as affinity strengths as a function of the solution conditions. As proteins comprise hydrophobic domains and charged moieties, and will also experience in-plane versus out-of-plane rotations and multipoint versus single-point adsorption/desorption during interaction with surfaces, our findings are valuable, especially since the rotational dynamics of pure proteins are still too fast to be imaged in real time and could only be studied by simulations thus far. Similar experiments

with different protein coatings, molecular-attachment strategies, solution conditions, and surface chemistries can be performed in the future to address important interfacial issues in various fields.

Received: January 2, 2014

Revised: April 9, 2014

Published online: May 14, 2014

Keywords: chromatography · gold nanorods · hydrophobic interactions · liquid/solid interfaces · single-particle rotational tracking

- [1] a) A. E. Nel, L. Madler, D. Velegol, T. Xia, E. M. V. Hoek, P. Somasundaran, F. Klaessig, V. Castranova, M. Thompson, *Nat. Mater.* **2009**, *8*, 543–557; b) D. J. Niedzwiecki, J. Grazul, L. Movileanu, *J. Am. Chem. Soc.* **2010**, *132*, 10816–10822; c) N. Schwierz, D. Horinek, S. Liese, T. Pirzer, B. N. Balzer, T. Hugel, R. R. Netz, *J. Am. Chem. Soc.* **2012**, *134*, 19628–19638.
- [2] a) M. J. Wirth, M. A. Legg, *Annu. Rev. Phys. Chem.* **2007**, *58*, 489–510; b) E. S. Yeung, *Annu. Rev. Phys. Chem.* **2004**, *55*, 97–126.
- [3] a) G. A. Myers, D. A. Gacek, E. M. Peterson, C. B. Fox, J. M. Harris, *J. Am. Chem. Soc.* **2012**, *134*, 19652–19660; b) M. Kastantin, R. Walder, D. K. Schwartz, *Langmuir* **2012**, *28*, 12443–12456.
- [4] a) M. E. Montgomery, M. A. Green, M. J. Wirth, *Anal. Chem.* **1992**, *64*, 1170–1175; b) M. J. Wirth, J. D. Burbage, *Anal. Chem.* **1991**, *63*, 1311–1317.
- [5] J. T. McCue in *Guide to Protein Purification*, 2nd ed., Vol. 463 (Eds.: R. R. Burgess, M. P. Deutscher), Academic Press, San Diego, **2009**, pp. 405–414.
- [6] L. Zhang, Y. Sun, *Biochem. Eng. J.* **2010**, *48*, 408–415.
- [7] a) C. Sönnichsen, A. P. Alivisatos, *Nano Lett.* **2005**, *5*, 301–304; b) D. Spetzler, J. York, D. Daniel, R. Fromme, D. Lowry, W. Frasch, *Biochemistry* **2006**, *45*, 3117–3124; c) P. Zijlstra, M. Orrit, *Rep. Prog. Phys.* **2011**, *74*, 0.
- [8] a) W. S. Chang, J. W. Ha, L. S. Slaughter, S. Link, *Proc. Natl. Acad. Sci. USA* **2010**, *107*, 2781–2786; b) G. Wang, W. Sun, Y. Luo, N. Fang, *J. Am. Chem. Soc.* **2010**, *132*, 16417–16422; c) L. H. Xiao, Y. X. Qiao, Y. He, E. S. Yeung, *J. Am. Chem. Soc.* **2011**, *133*, 10638–10645; d) L. H. Xiao, L. Wei, C. Liu, Y. He, E. S. Yeung, *Angew. Chem.* **2012**, *124*, 4257–4260; *Angew. Chem. Int. Ed.* **2012**, *51*, 4181–4184.
- [9] a) H. Yang, *J. Phys. Chem. A* **2007**, *111*, 4987–4997; b) D. Xu, Y. He, E. S. Yeung, *Anal. Chem.* **2014**, *86*, 3397–3404.
- [10] R. Ueberbacher, A. Rodler, R. Hahn, A. Jungbauer, *J. Chromatogr. A* **2010**, *1217*, 184–190.
- [11] R. W. Deitcher, J. P. O’Connell, E. J. Fernandez, *J. Chromatogr. A* **2010**, *1217*, 5571–5583.
- [12] L. Wang, J. Li, J. Pan, X. Jiang, Y. Ji, Y. Li, Y. Qu, Y. Zhao, X. Wu, C. Chen, *J. Am. Chem. Soc.* **2013**, *135*, 17359–17368.
- [13] X. H. N. Xu, E. S. Yeung, *Science* **1998**, *281*, 1650–1653.
- [14] Y. Gu, W. Sun, G. F. Wang, M. T. Zimmermann, R. L. Jernigan, N. Fang, *Small* **2013**, *9*, 785–792.